Clemson University
TigerPrints

Publications | Physics and Astronomy

3-1-1999

Beryllium Abundances in Halo Stars from Keck/ HIRES Observations

Ann Merchant Boesgaard
University of Hawaii

Constantine P. Deliyannis
Indiana University

Jeremy R. King
Clemson University, jking2@clemson.edu

Sean G. Ryan
Anglo-Australian Observatory

Steven S. Vogt
University of California

See next page for additional authors

Follow this and additional works at: https://tigerprints.clemson.edu/physastro_pubs

Recommended Citation
Please use publisher's recommended citation.

This Article is brought to you for free and open access by the Physics and Astronomy at TigerPrints. It has been accepted for inclusion in Publications by an authorized administrator of TigerPrints. For more information, please contact kokeefe@clemson.edu.

Authors
Ann Merchant Boesgaard, Constantine P. Deliyannis, Jeremy R. King, Sean G. Ryan, Steven S. Vogt, and Timothy C. Beers

This article is available at TigerPrints: https://tigerprints.clemson.edu/physastro_pubs/274

THE ASTRONOMICAL JOURNAL, 117:1549–1562, 1999 March
© 1999. The American Astronomical Society. All rights reserved. Printed in U.S.A.

BERYLLIUM ABUNDANCES IN HALO STARS FROM KECK/HIRES OBSERVATIONS

ANN MERCHANT BOESGAARD[1]
Institute for Astronomy, University of Hawaii at Mānoa, 2680 Woodlawn Drive, Honolulu, HI 96822; boes@ifa.hawaii.edu
CONSTANTINE P. DELIYANNIS[1]
Department of Astronomy, Indiana University, Swain Hall West, Bloomington, IN 47405; con@athena.astro.indiana.edu
JEREMY R. KING[1]
Space Telescope Science Institute, 3700 San Martin Drive, Baltimore, MD 21218; jking@stsci.edu
SEAN G. RYAN
Anglo-Australian Observatory, Epping, NSW 2121, Australia; and Royal Greenwich Observatory, sgr@ast.cam.ac.uk
STEVEN S. VOGT[1]
UCO/Lick Observatory, University of California at Santa Cruz, Santa Cruz, CA 95064; vogt@helios.ucsc.edu
AND
TIMOTHY C. BEERS[1]
Department of Physics and Astronomy, Michigan State University, East Lansing, MI 48824; beers@pa.msu.edu
Received 1998 October 5; accepted 1998 December 1

ABSTRACT

We have determined the abundance of Be in stars with an array of metal abundances in order to enhance our understanding of the chemical evolution of the Galaxy, cosmic-ray theory, and cosmology. Observations of the Be II resonance lines at λ3130 and λ3131 were made at the Keck telescope with the HIRES spectrometer at a resolution of 46,000 and signal-to-noise ratios of 60–110 (per pixel) typically. Our sample includes 22 halo dwarfs and five disk stars (including the Sun). We have taken special care in determining the stellar parameters for these stars in a consistent manner. The Be abundances were found (1) from the measured equivalent width of the relatively unblended Be II line at 3131.065 Å with an analysis that included 11 weak atomic and molecular lines near that wavelength and (2) from spectrum synthesis that included newly derived enhanced O (relative to Fe) in the synthesis calculations. The two methods are in excellent agreement. We find straight-line fits between Be and Fe:

$$\log N(\mathrm{Be/H}) = 0.96(\pm 0.04)[\mathrm{Fe/H}] - 10.59(\pm 0.03)\ ;$$

and between Be and O:

$$\log N(\mathrm{Be/H}) = 1.45(\pm 0.04)[\mathrm{O/H}] - 10.69(\pm 0.04)\ .$$

It seems that Be and Fe increase at the same rate during the course of the evolution of the Galaxy. But as O increases by a factor of 100, Be increases more rapidly, by a factor of 800. Traditional models in which energetic cosmic rays interact with ambient CNO nuclei in the interstellar medium to produce Be are consistent with this finding, as long as certain chemical evolution effects (such as mass outflow from the halo) are taken into account. However, models predicting a linear relationship between Be and O, such as those producing Be in the vicinity of Type II supernovae, are less consistent with our result. There is some evidence for an intrinsic spread in Be at a given [Fe/H] or [O/H]. There is currently no evidence of a primordial plateau level of Be down to $\log N(\mathrm{Be/H}) = -13.5$.

Key words: Galaxy: evolution — Galaxy: halo — stars: abundances — stars: atmospheres — stars: Population II

1. INTRODUCTION

Knowledge of the origin and evolution of Be in the Galaxy will enhance our understanding of the chemical history of the Galaxy, cosmic-ray theory, cosmology, and possibly big bang nucleosynthesis (BBN). Unlike the heavier elements, which are formed by nuclear fusion in the high-temperature interiors of stars, Be is destroyed in stellar interiors. It is widely accepted that Be is created by interactions of high-energy cosmic rays ($\mathrm{H\&He_{CR}}$) with abundant elements such as C, N, O in the interstellar gas ($\mathrm{CNO_{ISM}}$) as first proposed by Reeves, Fowler, & Hoyle (1970); whether these interactions take place in the immediate vicinity of supernovae or in the general interstellar gas is not completely clear. (Some evidence from Be and B points to the former locale [Duncan et al. 1997].) In the early Galaxy, there was little $\mathrm{CNO_{ISM}}$ but plenty of $\mathrm{CNO_{CR}}$, and this reaction was of greater *relative* importance then than now (Yoshii, Kajino, & Ryan 1997). It also gives a first-order rather than a quadratic dependence of Be on Fe. The evolution of the abundance of Be should reflect the production of CNO and cosmic rays and thus mirror the production of massive stars (which contribute the O atoms) and supernovae.

The study of Be in the oldest stars may reveal if any Be has been synthesized in the big bang. The standard model of BBN has had remarkable success in predicting abundances for the light isotopes of ^{2}H, ^{3}He, ^{4}He, and ^{7}Li that are in

[1] Visiting Astronomer, W. M. Keck Observatory, jointly operated by the California Institute of Technology and the University of California.

TABLE 1

STARS OBSERVED FOR Be

Star	V	U	$B-V$	Night[a]	Exposure Time (minutes)	Total	S/N	Equivalent Width (mÅ)
HD 19445	8.05	8.28	0.46	1	20	20	88	9.7
HD 64090	8.31	8.79	0.62	1	20	20	77	22.4
HD 74000	9.67	9.84	0.42	11	60	60	44	21.2
HD 76932	5.83	6.45	0.53	7	10	10	110	82.7
HD 84937	8.31	8.48	0.39	3	45	45	98	4.8
HD 94028	8.23	8.43	0.47	11	20	20	60	49.2
HD 103095	6.45	7.37	0.75	4	15	15	81	9.2
HD 134169	7.69	8.12	0.53	10	25	25	62	82.5
HD 140283	7.21	7.50	0.49	3	60	60	164	8.2
HD 184499	6.61	7.19	0.58	1	25	25	109	91.6
HD 194598	8.35	8.66	0.48	7	60	60	67	33.1
HD 201889	8.06	8.61	0.59	8	30	30	75	83.2
HD 219617	8.16	8.45	0.49	7	30	30	67	18.4
BD +37°1458.....	8.92	9.41	0.60	11	75	75	76	12.7
BD +26°3578.....	9.36	9.53	0.39	5	90	90	88	6.6
BD +23°3912.....	8.88	9.33	0.51	1	30			
				2	30	60	66	51.8
BD +20°3603.....	9.75	9.53	0.39	6	60			
				11	95	155	90	10.2
BD +17°4708.....	9.47	9.70	0.44	7	90	90	73	21.5
BD +03°740	9.81	9.97	0.36	2	165			
				3	75			
				7	120			
				8	120			
				9	120	600	176	2.7
BD +02°3375.....	9.92	10.14	0.44	5	90	90	63	8.0
BD −04°3208.....	10.02	10.22	0.40	5	87	87	56	7.3
BD −13°3442.....	10.26	10.46	0.40	3	165			
				10	260			
				11	240	665	129	2.0
HR 2943	0.37	0.81	0.37	2	1	1	500	<1
HR 3775	3.17	3.66	0.46	3	3	3	95	102.8
HR 5927	6.31	6.80	0.49	6	7	7	61	99.3
HR 8430	3.77	4.18	0.43	12	5	5	119	86.0
HR 8888	6.62	6.99	0.36	13	40	40	61	89.0
Sun	...	...	...	2	20	20	138	76.1

[a] 1 = 1993 Oct 6; 2 = 1993 Oct 7; 3 = 1994 Mar 1; 4 = 1994 Apr 28 (service); 5 = 1994 Jun 12; 6 = 1994 Jul 5; 7 = 1994 Oct 26; 8 = 1994 Oct 27; 9 = 1994 Nov 27; 10 = 1995 Mar 14; 11 = 1995 Mar 15; 12 = CFHT, 1990 Oct 3; 13 = CFHT, 1995 Oct 16.

agreement with the observed or inferred primordial abundances resulting in similar values for the universal baryon density (Boesgaard & Steigman 1985; Deliyannis et al. 1989; Walker et al. 1991; Copi, Schramm, & Turner 1995). Very little Be [N(Be)/N(H) = 10^{-17}] is produced in standard BBN models (Thomas et al. 1994). There are several indications that standard BBN may be incomplete and that inhomogeneous BBN might be more appropriate. Witten (1984) has suggested that the quark-hadron phase transition preceding BBN must lead to inhomogeneities. Models that include inhomogeneities in the early universe could produce a different mixture of light elements than the standard models (see the review by Malaney & Mathews 1992). Beryllium is a particularly good diagnostic as inhomogeneous models can create far more Be than the standard model does. At first, it was thought that N(Be)/N(H) might be as high as 10^{-13} (Malaney & Fowler 1989), though various improvements in the physics imply that 10^{-15} to 10^{-14} might be a more realistic upper limit (Orito et al. 1997). This is still far above the standard value of 10^{-17}. Inhomogeneous models also produce a higher primordial Li abundance, though more Be does not necessarily imply more Li as well.

Several groups have determined Be abundances in halo stars including Rebolo et al. (1988), Ryan et al. (1990), Gilmore, Edvardsson, & Nissen (1991), Ryan et al. (1992), Gilmore et al. (1992), Boesgaard & King (1993), and Molaro et al. (1997). The last four papers show straight-line fits between Be and Fe and seemingly between Be and O also. Such a linear relationship seems to indicate that the environment for the spallation reactions is the vicinity of supernovae (SN II's) with freshly minted CNO nuclei rather than the ambient interstellar medium. In the extreme case, a quadratic relationship between Be and Fe would be expected if the CNO atoms are proportional to the number of SN II's and the cosmic rays are proportional to the instantaneous rate of SN II production. However, chemical evolution complications, such as mass outflow from the halo, imply a more complex relationship; in particular, there will be a shallower slope with increasing metallicity. Several models have been presented to account for the production of the light elements in the early history of the

Galaxy by spallation reactions, e.g., Vangioni-Flam et al. (1990); Ryan et al. (1992); Prantzos, Cassé, & Vangioni-Flam (1993); Casuso & Beckman (1997); Lemoine, Vangioni-Flam, & Cassé (1998); and Vangioni-Flam et al. (1998). Prantzos et al. (1993) have presented a detailed chemical evolution model that includes parameters such as the cosmic-ray spectrum, the early star formation rate, the rate of supernovae, mass inflow and outflow, and metallicity distribution functions. The slope of the observed fits in the log N(Be/H) versus [Fe/H] plane or log N(Be/H) versus [O/H] plane are good diagnostics to narrow the parameter space. The slopes of the fits may change for different metallicity regimes as suggested by Deliyannis et al. (1995) and Molaro et al. (1997) for [Fe/H] < -1.4. Malaney & Butler (1993) have applied realistic nuclear physics that suggests that the slope of the Be-Fe relation will be steeper at [Fe/H] < -3.0 than for higher metallicities. These models provide the framework in which to interpret Be observations.

In this work we have been able to reach some especially low metallicity stars that are faint and required long exposures even with the largest telescope in the world. We have observed stars with [Fe/H] values of < -2.5 to search for a Be plateau that might indicate a BBN component of Be. In the most metal-poor stars the Be II lines are expected to be very weak so high-resolution and high signal-to-noise ratio (S/N) spectroscopy are needed. We have observed Be in stars with an array of metallicities to investigate the galactic evolution of Be. To this end we have also determined O abundances in these stars (Boesgaard et al. 1999) and thus have a consistently determined data set of Be and O abundances in halo stars. A preliminary report on a subset of these stars was presented by Boesgaard (1996). We show in this study that Be abundances can be determined to a precision of ± 0.1 dex and that Be is highly correlated with both Fe and O.

2. OBSERVATIONS

Observations of Be are from the Be II resonance lines at 3130.420 and 3131.065 Å in the ultraviolet (UV) spectral region accessible from the ground. This wavelength is near the atmospheric cutoff, and more UV flux penetrates the atmosphere at the altitude of Mauna Kea than at other ground-based observatories. To maximize the UV flux, we have made observations as close as possible to the lowest air mass for each star. We report here on Keck observations of 22 metal-poor stars taken from five different observing runs plus one service observation obtained for us. We also took exposures of the daytime sky, as a solar spectrum, and of three disk stars for comparison with the halo stars. We include data on two other disk stars that have near-solar values of Be, Fe, and O.

Metal-poor stars in the temperature regime of our program stars ($T_{\rm eff}$ = 5100–6300) are faint at the Be II wavelengths, so the light-gathering power of the Keck telescope was important to achieve both high resolution and high S/Ns. We used the HIRES spectrometer (Vogt et al. 1994) on the Keck I telescope. The detector was a Tektronix 2048^2 CCD with a quantum efficiency near 3130 Å of only about 7%. The resolution of the spectra is $\sim$46,000 (FWHM = 3 pixels) with an effective dispersion of 0.022 Å pixel^{-1}. The wavelength coverage was typically 3100–3150 Å in the order of interest. We kept our exposure times to 30–40 minutes maximum to limit the cosmic-ray hits that might affect the spectra; we co-added multiple spectra from a given night, a given run, or from different runs. On each night one to three Th-Ar comparison spectra were taken, usually at the beginning and the end of the night. There were 10–18 flat-field exposures taken each night with exposure times of 250–300 s each to obtain sufficient counts at 3130 Å. In addition between four and 11 bias frames were obtained each night.

The observations are presented in Table 1, which gives the star names, the V and U magnitudes, $B-V$, the observing run dates, the individual exposures, the total exposure time, and the total S/N per pixel in the Be order. The last column contains the equivalent width of the Be II line at λ3131 (see below).

3. STELLAR DATA AND ANALYSIS

3.1. *Data Reduction*

Standard echelle reductions were carried out within the IRAF routines and have been described in Boesgaard et al. (1999). The multiple flat-field and bias frames were combined to produce a nightly master flat and master bias frame that were applied to the stellar frames. The severe cosmic-ray hits on the CCD were identified manually and removed using the IRAF FIXPIX task. The dispersion solutions were made from the ThAr nightly comparison spectra from low-order Legendre polynomial fits to hundreds of lines. With a dispersion in the Be II order of 0.022 pixel^{-1} and a measured FWHM for the comparison lines of approximately 3.1 pixels, the effective resolution is $\sim$46,000. In order to co-add the spectra from different times of night or from different nights/runs, the cross-correlation techniques in IRAF were used to determine the spectral shifts.

The continua were fitted quite easily for the lowest metallicity stars since the blending features in this crowded spectral region are so weak. The spectra of these stars could be used to help identify the continuum high points in the stars with progressively stronger atomic and molecular features. Examples of the spectra over a short region near the Be II lines of four stars covering a range in [Fe/H] are shown in Figure 1. The stars are shown in decreasing order of [Fe/H], and increasing temperature, from Figure 1*a* to Figure 1*d*.

3.2. *Stellar Parameters*

We followed the technique used in Deliyannis et al. (1999, hereafter DBKD) to determine stellar parameters in a self-consistent way. (An abbreviated discussion of this appears in Boesgaard et al. 1999.) We have chosen to use two different temperature scales: one that has been used widely, essentially that of Carney (1983b), and one that is more consistent with the Balmer line temperatures and the photometric temperatures of Fuhrmann, Axer, & Gehren (1995) and Gratton, Carretta, & Castelli (1996), essentially that of King (1993). One to four Balmer lines were used by Fuhrmann et al. to find temperatures of more than 100 dwarfs and subgiants of a wide range of metallicities; these temperatures, like those of King (1993), are generally $\sim$100 K hotter than those on the Carney (1983b) scale.

The temperature indicators used are $b-y$, $V-K$, and $R-I$. The Strömgren photometry is from Schuster & Nissen (1988); values for $V-K$ are from Carney (1983a, 1983b), Laird, Carney, & Latham (1988), and B. W. Carney (1993, private communication); the $R-I$ values are from

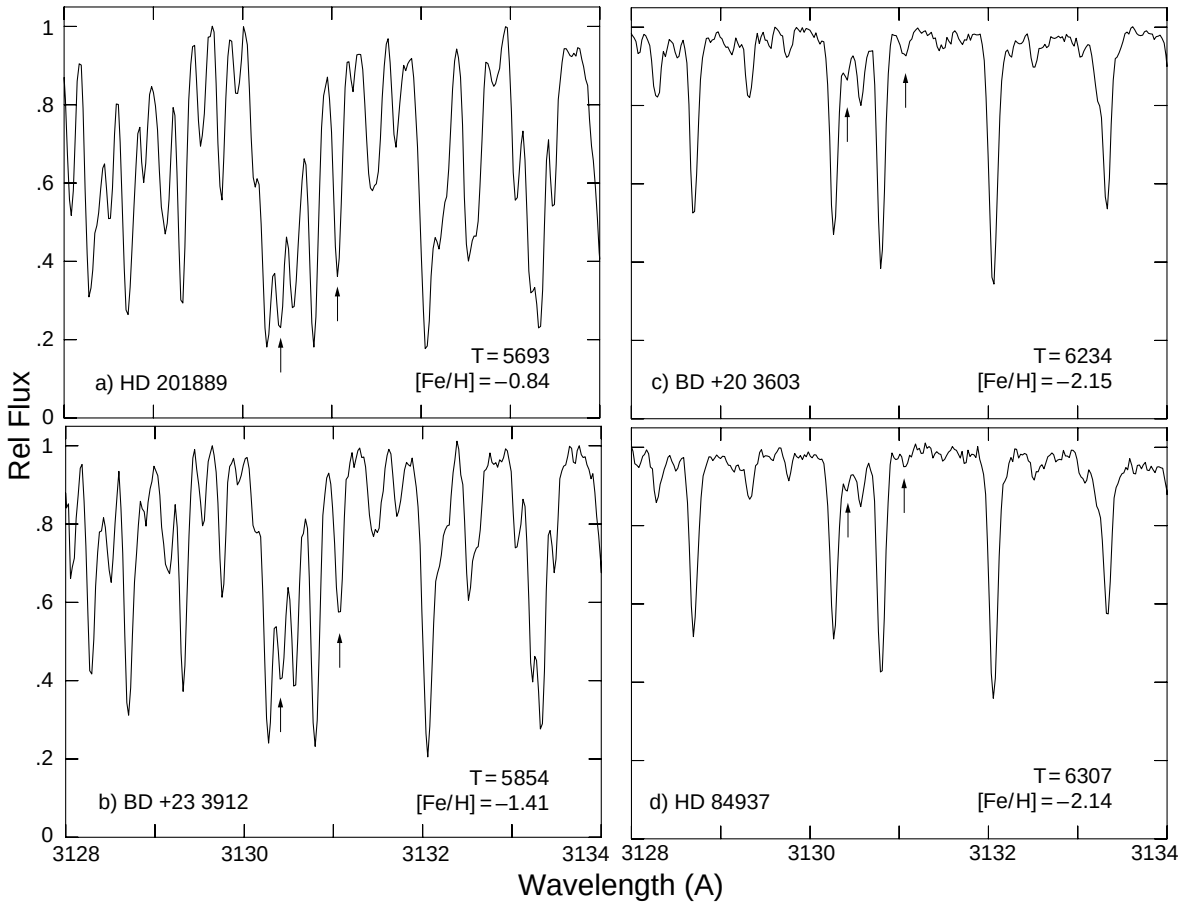

FIG. 1.—Six Å of the spectra in the Be II region of four stars, shown in order of decreasing [Fe/H] and increasing temperature. Small arrows indicate the positions of the two Be II features. The stellar parameters for HD 84937 and BD +20°3603 are very similar, yet the Be line at λ3131 is twice as strong in BD +20°3603. The values for T and [Fe/H] are on the King scale.

Laird (1985), Ryan (1989), Carney & Aaronson (1979), Carney (1980, 1983a), and Eggen (1978). As in DBKD, we apply corrections for interstellar reddening where needed and use $E(b-y)$ from Shuster & Nissen as the primary source to estimate reddening. For the other color indices, the Johnson (1968) relations were used: $E(V-K) = 3.75E(b-y)$ and $E(R-I) = 1.08E(b-y)$. The temperatures derived from the photometry were weighted 4:2:1 for $T(b-y)$, $T(V-K)$, and $T(R-I)$, except for the coolest stars, where we used 3:3:1. The error from the standard deviation of the weighted mean is typically 40 K.

The values for [Fe/H] were taken from high spectral resolution determinations in the literature. These were (1) corrected to a solar value of log $N(\mathrm{Fe/H}) + 12.0 = 7.51$ (Anders & Grevesse 1989) and (2) corrected for the temperature difference between the published values and our scale. Since the King scale is somewhat hotter ($\sim$100 K), it gives somewhat higher values for [Fe/H]. The mean error in the determinations of [Fe/H] is 0.14 dex.

One of the methods we employed to find gravities was to use published detailed analyses that used ionization balance to find log g, e.g., Magain (1989), Gratton & Sneden (1988), and Tomkin et al. (1992). We derived revised log g values to account for our values of temperature and [Fe/H]. We also used two other methods, one involving the Strömgren diagrams of c_0 versus $(b-y)_0$ and the other a comparison of theoretical isochrones in the log g versus T_{eff} plane. More discussion of this appears in DBKD and Boesgaard et al. (1999). The mean error in log g is 0.22 dex. We have used the Magain (1987) value for microturbulence for Population II stars of $\xi = 1.5$ km s^{-1}.

In Tables 2 and 3 we give the derived stellar parameters for the two temperature scales and the individual errors on each parameter for each star. We have invested much effort in the determination of these parameters so that they are as self-consistent as possible. We have done detailed abundance analyses on each star with each of the sets of parameters and examine the dependence of our results on the stellar model inputs.

4. ABUNDANCE DETERMINATIONS

We have determined abundances both from spectrum syntheses and from the measured equivalent widths of Be II lines. In each method the results from the weaker, less blended line at 3131 Å are to be preferred. R. L. Kurucz (1993, private communication) model atmospheres have been used throughout.

4.1. *Equivalent Width Method*

We have measured the equivalent width of the Be II line at λ3131 for all the stars, usually by fitting it with a Gaussian in the IRAF splot package. Figure 2 shows examples of the Gaussian fit in six stars in order of decreasing metallicity. The stronger Be II line at λ3130 could be seen distinctly in some of the stars (see Figs. 1 and 2), and its equivalent width could be determined with IRAF deblend-

TABLE 2

STELLAR PARAMETERS ON THE KING (1993) SCALE

Star	$T_{\rm eff}$ (K)	σ	log g	σ	[Fe/H]	σ
HD 19445	5996	52	4.48	0.13	−2.01	0.08
HD 64090	5478	40	4.70	0.27	−1.67	0.15
HD 74000	6249	40	4.33	0.10	−1.99	0.12
HD 76932	5943	80	4.07	0.10	−0.87	0.09
HD 84937	6307	40	4.00	0.10	−2.14	0.14
HD 94028	6043	40	4.45	0.18	−1.46	0.08
HD 103095	5133	40	4.75	0.10	−1.26	0.20
HD 134169	5900	40	3.74	0.24	−0.85	0.08
HD 140283	5847	40	3.63	0.20	−2.46	0.14
HD 184499	5670	40	4.00	0.20	−0.51	0.14
HD 194598	6042	40	4.36	0.10	−1.16	0.19
HD 201889	5693	40	3.81	0.31	−0.84	0.26
HD 219617	6011	40	4.42	0.26	−1.49	0.21
BD +37°1458.....	5554	48	3.62	0.12	−2.06	0.18
BD +26°3578.....	6269	51	4.04	0.22	−2.24	0.11
BD +23°3912.....	5854	40	3.84	0.10	−1.41	0.16
BD +20°3603.....	6234	76	4.33	0.26	−2.15	0.16
BD +17°4708.....	6091	57	3.81	0.19	−1.73	0.10
BD +03°740	6227	60	3.75	0.27	−2.81	0.09
BD +02°3375.....	5949	40	4.17	0.30	−2.30	0.11
BD −04°3208.....	6401	113	3.94	0.34	−2.31	0.21
BD −13°3442.....	6273	53	3.60	0.55	−2.94	0.08
HR 3775	6300	40	4.10	0.20	−0.17	0.10
HR 5927	6377	53	4.00	0.20	+0.05	0.10
HR 8430	6488	69	4.10	0.20	−0.08	0.10
HR 8888	6722	46	4.10	0.20	+0.01	0.10
Sun	5770	...	4.44	...	0.00	0.04

TABLE 3

STELLAR PARAMETERS ON THE CARNEY (1983b) SCALE

Star	$T_{\rm eff}$ (K)	σ	log g	σ	[Fe/H]	σ
HD 19445	5852	40	4.41	0.23	−2.10	0.12
HD 64090	5341	40	4.73	0.10	−1.77	0.18
HD 74000	6134	40	4.26	0.10	−2.05	0.12
HD 76932	5807	40	4.00	0.12	−0.95	0.11
HD 84937	6206	40	3.89	0.13	−2.20	0.14
HD 94028	5907	64	4.44	0.17	−1.54	0.09
HD 103095	5007	40	4.65	0.15	−1.37	0.18
HD 134169	5759	82	3.68	0.16	−0.94	0.05
HD 140283	5692	40	3.47	0.13	−2.56	0.12
HD 184499	5670	40	4.00	0.15	−0.51	0.14
HD 194598	5911	42	4.32	0.13	−1.25	0.16
HD 201889	5553	41	3.74	0.24	−0.95	0.26
HD 219617	5872	40	4.52	0.15	−1.58	0.16
BD +37°1458.....	5408	40	3.41	0.26	−2.14	0.17
BD +26°3578.....	6158	64	3.94	0.12	−2.32	0.15
BD +23°3912.....	5691	40	3.68	0.10	−1.53	0.15
BD +20°3603.....	6114	89	4.27	0.20	−2.22	0.16
BD +17°4708.....	5956	62	3.65	0.26	−1.81	0.10
BD +03°740	6110	82	3.64	0.33	−2.89	0.09
BD +02°3375.....	5800	40	4.07	0.41	−2.39	0.17
BD −04°6316.....	6316	121	3.90	0.42	−2.35	0.20
BD −13°3442.....	6159	40	3.50	0.44	−3.02	0.16
HR 3775	6300	40	4.10	0.20	−0.17	0.10
HR 5927	6377	53	4.00	0.20	+0.05	0.10
HR 8430	6488	69	4.30	0.20	−0.08	0.10
HR 8888	6722	46	4.00	0.20	+0.01	0.10
Sun	5770	...	4.44	...	0.00	0.04

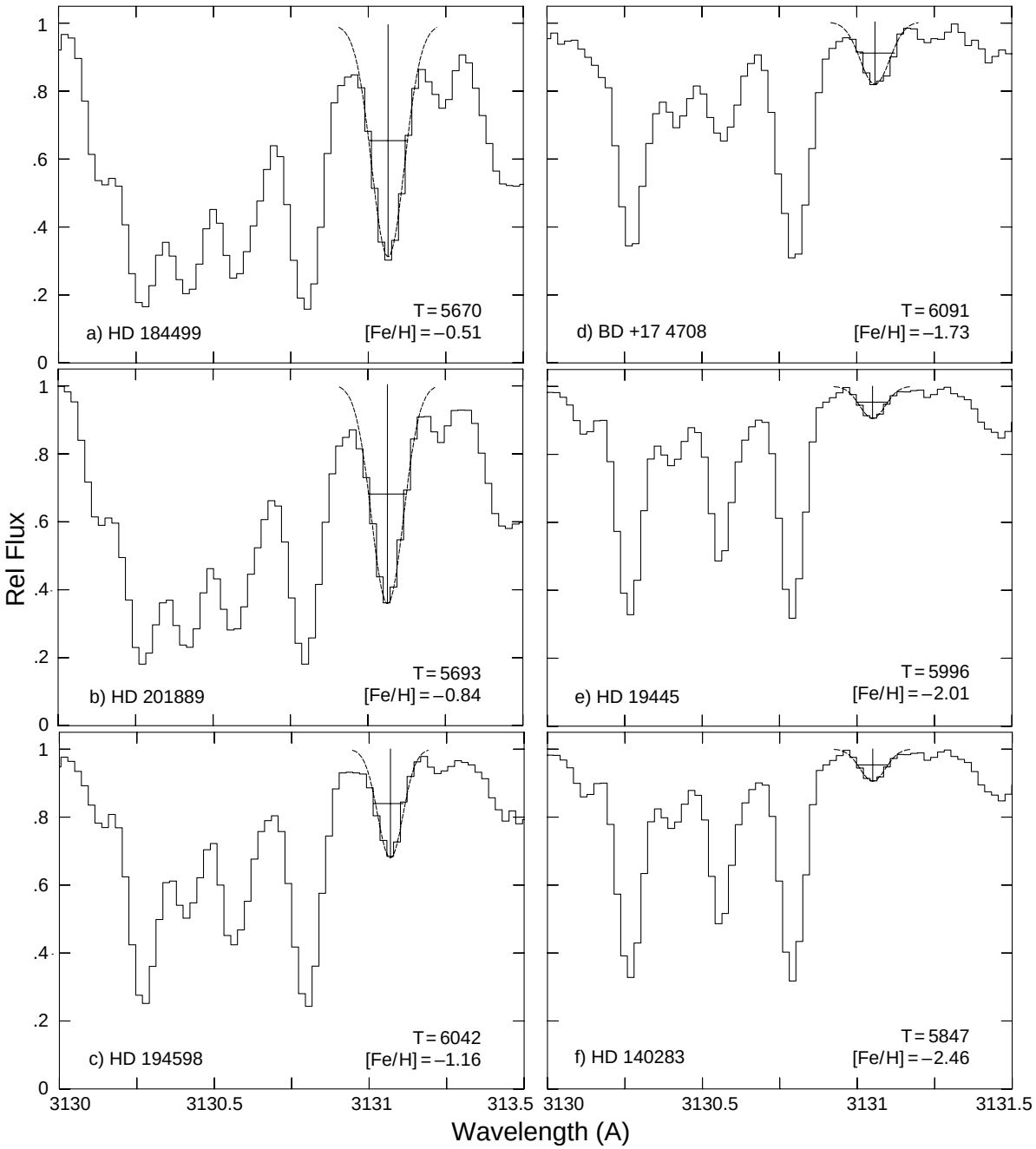

FIG. 2.—Histogram IRAF plots of a 1.5 Å region of the Be II lines for six stars showing the Gaussian profile fit to the λ3131 line. These spectra are in order of decreasing stellar [Fe/H] from −0.5 to −2.5 and decreasing Be equivalent width from 92 to 8 mÅ. The values for T and [Fe/H] are on the King scale.

ing techniques. However, this second line serves more to verify the presence of Be II, particularly in the weak-Be stars, than to provide an abundance determination. We found that the line appeared at the correct wavelength and at the correct ratio of the gf-values (2 to 1). The measured equivalent widths of the λ3131 feature is given for each star in the right-hand column of Table 1.

We have determined Be abundances with the line analysis program MOOG (Sneden 1973). We treated the λ3131.065 Be II line as a blend with 11 other atomic and molecular lines between 3131.015 and 3131.116 Å from the line list of King, Deliyannis, & Boesgaard (1997) as weak possible blends. This shortened line list is given in Table 4. The Be abundances from this method are given in the second column of Tables 5 and 6.

Most previous studies of Be do not give the equivalent width of either Be II line, which makes it difficult to compare our results directly with theirs. Owing to the complex dependence of the ionization of Be I on $T_{\rm eff}$ and log g in this region of the stellar parameter space (as discussed in § 4.3), it is not easy to extract the equivalent widths of others from their abundances or to make a simple transformation from published abundances to what those abundances would be with our parameters. One comparison that can be made is with the data in Boesgaard & King (1993). The mean difference between our high-resolution equivalent widths for the

TABLE 4

LINES IN THE Be II λ3131 REGION USED IN THE Be BLEND

Wavelength (Å)	Feature	Excitation Potential	*gf* Value	Dissociation Potential
3131.015.....	Mn II	6.11	4.100×10^{-2}	
3131.034.....	CN	1.83	3.184×10^{-3}	7.76
3131.037.....	Mn I	3.77	1.884×10^{-2}	
3131.058.....	CH	0.03	4.000×10^{-3}	3.46
3131.059.....	Mn II	6.67	1.910×10^{-3}	
3131.063.....	V II	4.24	2.871×10^{-5}	
3131.065.....	Be II	0.00	3.404×10^{-1}	
3131.069.....	CN	2.36	5.445×10^{-3}	7.76
3131.074.....	CH	2.34	3.062×10^{-1}	3.46
3131.074.....	CN	1.66	8.318×10^{-4}	7.76
3131.076.....	CN	1.57	2.636×10^{-4}	7.76
3131.109.....	Zr I	0.52	3.981×10^{-1}	
3131.115.....	Fe I	3.05	1.936×10^{-6}	
3131.115.....	NH	1.38	2.361×10^{-3}	3.47

Be II λ3131 line and theirs for the 12 stars in common is -2 ± 11 mÅ.

4.2. *Spectrum Synthesis Method with Enhanced Oxygen*

In the spectrum synthesis we have combined the Be line lists of Ryan et al. (1992) and King et al. (1997), which originally came from R. L. Kurucz (1993, private communication: CD-ROM 15). The range in the stellar temperatures in this sample and the high S/N ratios of the spectra allowed clarification of certain odd line behaviors, and some minor adjustments were made to the line list. The Keck spectrum of Procyon could be used to investigate the atomic lines because the molecular lines are virtually absent in Procyon. Two models were used, that of Steffen (1985) and that of Tomkin & Lambert (1978). Only the longward Be II line could be used to set an upper limit to the Be abundance. This star is very Be-deficient, and a weak CH line is present near the expected position of the Be line. The *gf*-value for one notable, blending line at λ3131.058 due to CH was reduced to 4.0×10^{-3}.

For the Sun we used the solar spectrum from the solar flux atlas (Kurucz et al. 1984) and the Kurucz solar model. The abundance from the longward line is weighted twice the shortward line for the solar Be abundance. The Be abun-

TABLE 5

BERYLLIUM ABUNDANCES ON THE KING (1993) SCALE

Star	log *N*(Be/H) (eqw)	log *N*(Be/H) (syn)	σ	[Fe/H]	σ	[O/H]	σ
HD 19445	−12.46	−12.45	0.06	−2.01	0.08	−1.23	0.08
HD 64090	−12.19	−12.17	0.13	−1.67	0.15	−1.10	0.10
HD 74000	−12.03	−12.38	0.06	−1.99	0.12	−1.44	0.05
HD 76932	−11.17	−11.17	0.05	−0.87	0.09	−0.43	0.09
HD 84937	−12.85	−12.83	0.07	−2.14	0.14	−1.35	0.06
HD 94028	−11.51	−11.51	0.08	−1.46	0.08	−0.87	0.08
HD 103095	−12.00	−11.70	0.08	−1.26	0.20	−0.88	0.11
HD 134169	−11.32	−11.32	0.10	−0.85	0.08	−0.40	0.10
HD 140283	−12.95	−13.08	0.09	−2.46	0.14	−1.60	0.07
HD 184499	−10.97	−10.97	0.09	−0.51	0.14	−0.20	0.09
HD 194598	−11.81	−11.73	0.05	−1.16	0.19	−0.69	0.06
HD 201889	−11.30	−11.32	0.13	−0.84	0.26	−0.38	0.06
HD 219617	−12.15	−12.13	0.12	−1.49	0.21	−0.82	0.09
BD 37°1458	−12.90	−12.88	0.08	−2.06	0.18	−1.23	0.08
BD 26°3578	−12.70	−12.83	0.10	−2.24	0.11	−1.48	0.06
BD 23°3912	−11.79	−11.84	0.05	−1.41	0.16	−0.72	0.06
BD 20°3603	−12.40	−12.54	0.11	−2.15	0.16	−1.38	0.12
BD 17°4708	−12.28	−12.29	0.08	−1.73	0.10	−0.95	0.07
BD 03°740.....	−13.24	−13.37	0.10	−2.81	0.09	−1.95	0.07
BD 02°3375	−12.70	−12.59	0.15	−2.30	0.11	−1.36	0.10
BD −04°3208.....	−12.63	−12.62	0.15	−2.31	0.21	−1.44	0.11
BD −13°3442.....	−13.40	−13.50	0.21	−2.94	0.08	−1.75	0.12
HR 3775	−10.79	−10.79	0.09	−0.17	0.10	−0.01	0.10
HR 5927	−10.73	−10.73	0.08	+0.05	0.10	−0.05	0.08
HR 8430	−10.77	−10.77	0.09	−0.08	0.10	+0.02	0.10
HR 8888	−10.79	−10.79	0.08	+0.01	0.10	0.00	0.07
Sun	−10.89	−10.89	0.04	0.00	0.04	−0.04	0.04

TABLE 6

BERYLLIUM ABUNDANCES ON THE CARNEY (1983b) SCALE

Star	log N(Be/H) (eqw)	log N(Be/H) (syn)	σ	[Fe/H]	σ	[O/H]	σ
HD 19445	−12.55	−12.48	0.11	−2.10	0.12	−1.29	0.10
HD 64090	−12.49	−12.19	0.06	−1.77	0.18	−1.12	0.07
HD 74000	−12.10	−12.47	0.06	−2.05	0.12	−1.46	0.06
HD 76932	−11.24	−11.23	0.05	−0.95	0.11	−0.50	0.08
HD 84937	−12.94	−12.92	0.08	−2.20	0.14	−1.46	0.05
HD 94028	−11.55	−11.54	0.08	−1.54	0.09	−0.94	0.10
HD 103095	−12.04	−11.85	0.08	−1.37	0.18	−0.96	0.11
HD 134169	−11.40	−11.38	0.08	−0.94	0.05	−0.49	0.10
HD 140283	−13.08	−13.15	0.06	−2.56	0.12	−1.68	0.06
HD 184499	−10.97	−10.97	0.09	−0.51	0.14	−0.20	0.08
HD 194598	−11.88	−11.82	0.06	−1.25	0.16	−0.76	0.07
HD 201889	−11.36	−11.38	0.10	−0.95	0.26	−0.47	0.08
HD 219617	−12.15	−12.09	0.07	−1.58	0.16	−0.89	0.08
BD 37°1458	−13.07	−13.08	0.13	−2.14	0.17	−1.26	0.09
BD 26°3578	−12.79	−12.93	0.07	−2.32	0.15	−1.53	0.06
BD 23°3912	−11.92	−11.99	0.05	−1.53	0.15	−0.80	0.06
BD 20°3603	−12.47	−12.62	0.09	−2.22	0.16	−1.50	0.12
BD 17°4708	−12.40	−12.42	0.11	−1.81	0.10	−0.97	0.09
BD 03°740	−13.33	−13.47	0.14	−2.89	0.09	−2.04	0.12
BD 02°3375	−12.80	−12.63	0.18	−2.39	0.17	−1.45	0.11
BD −4°3208	−12.69	−12.68	0.16	−2.35	0.20	−1.49	0.11
BD −13°3442	−13.49	−13.59	0.18	−3.02	0.16	−1.81	0.12
HR 3775	−10.68	−10.79	0.09	−0.15	0.10	−0.01	0.10
HR 5927	−10.73	−10.73	0.08	+0.05	0.10	−0.05	0.08
HR 8430	−10.77	−10.77	0.09	−0.08	0.10	+0.02	0.10
HR 8888	−10.79	−10.79	0.08	+0.01	0.10	0.00	0.07
Sun	−10.89	−10.89	0.04	0.00	0.04	−0.04	0.04

dance of A(Be) = log N(Be/H) + 12.0 is 1.05, close to the solar value determined in the detailed analysis by Chmielewski, Brault, & Mueller (1975) of 1.11. We also have a Keck spectrum of the daytime sky; for this spectrum the abundance from only the λ3131 line gave A(Be) = 1.11.

The stellar models that we have used for our Be syntheses are Kurucz models for the specific values of $T_{\rm eff}$, log g, and [Fe/H]. The synthesis calculations have been modified to include the effect of enhanced O. Our study of O abundances in these same stars (Boesgaard et al. 1999) has enabled us to specify the O abundance. Instead of reducing all the heavy elements by the amount of [Fe/H], we have put in the derived amount of O. This is an important consideration because there are OH features in the Be blend.

Synthesis fits were made to all of the spectra with both sets of stellar parameters. Figure 3 shows a sample of the final fits for eight stars, six with the King parameters and two with the Carney. The Be abundance results from the syntheses are shown in the third column of Tables 5 and 6. The agreement between the abundances determined by the equivalent width method and by spectrum synthesis is very good; this is shown for the King-scale parameters in Figure 4.

4.3. *Beryllium Abundance Errors*

For each star there is an uncertainty associated with the parameters $T_{\rm eff}$, log g, and [Fe/H] as shown in Tables 2 and 3. There is also an uncertainty due to the placement of the continuum, which, in part, reflects the data quality as indicated by S/N ratios from Table 1. These can be translated into errors in the Be abundances. However, this is not the usual straightforward process of $\Delta T = X$ giving Δ log N(Be/H) = Y and Δ log $g = R$ giving Δ log N(Be/H) = S, and then adding Y and S in quadrature. As can be seen in Boesgaard & King (1993), in this temperature and log g regime, the Be abundance from Be II has a complex pattern. The values of the parameters, $T_{\rm eff}$, log g, and [Fe/H], influence the degree of ionization of Be I; Be II is dominant in our region of the parameter space. For various values of log g, the Be II equivalent width reaches a maximum at different temperatures. (See Boesgaard & King 1993, Figs. 4, 5, and 6 for examples of the intricacies of the mutual dependencies.)

Therefore, we have found the error for Be at a given temperature for the individual value for log g. For example, the error due to an uncertainty of 0.5 in log g at $T_{\rm eff}$ = 6200 K is 0.18 dex for log g = 3.85 and 0.20 dex for log g = 4.35. Similarly, the error due to an uncertainty of 100 K in $T_{\rm eff}$ at 6200 K is 0.04 dex at log g = 4.5 and 0.05 dex at log g = 4.0. The temperature uncertainties are typically 40–70 K, and the corresponding uncertainty in log N(Be/H) is 0.02–0.04 dex. The uncertainties in log g are typically 0.1–0.3 dex, which corresponds to an uncertainty in log N(Be/H) of 0.04–0.12. The estimated errors due to the placement of the continuum are typically 0.02–0.06. Inasmuch as we have found uncertainties by taking into account the mutual dependences, we are free to add the errors in quadrature. The final error estimates on log N(Be/H) are given in the fourth column of Tables 5 and 6.

4.4. *Comments: Notes on Individual Stars*

HD 19445.—The synthesis fits for this star are good with both sets of parameters, although the two Be lines agree with each other better for the cooler temperature of 5852 K. The spectrum can be seen in Figure 2*e*.

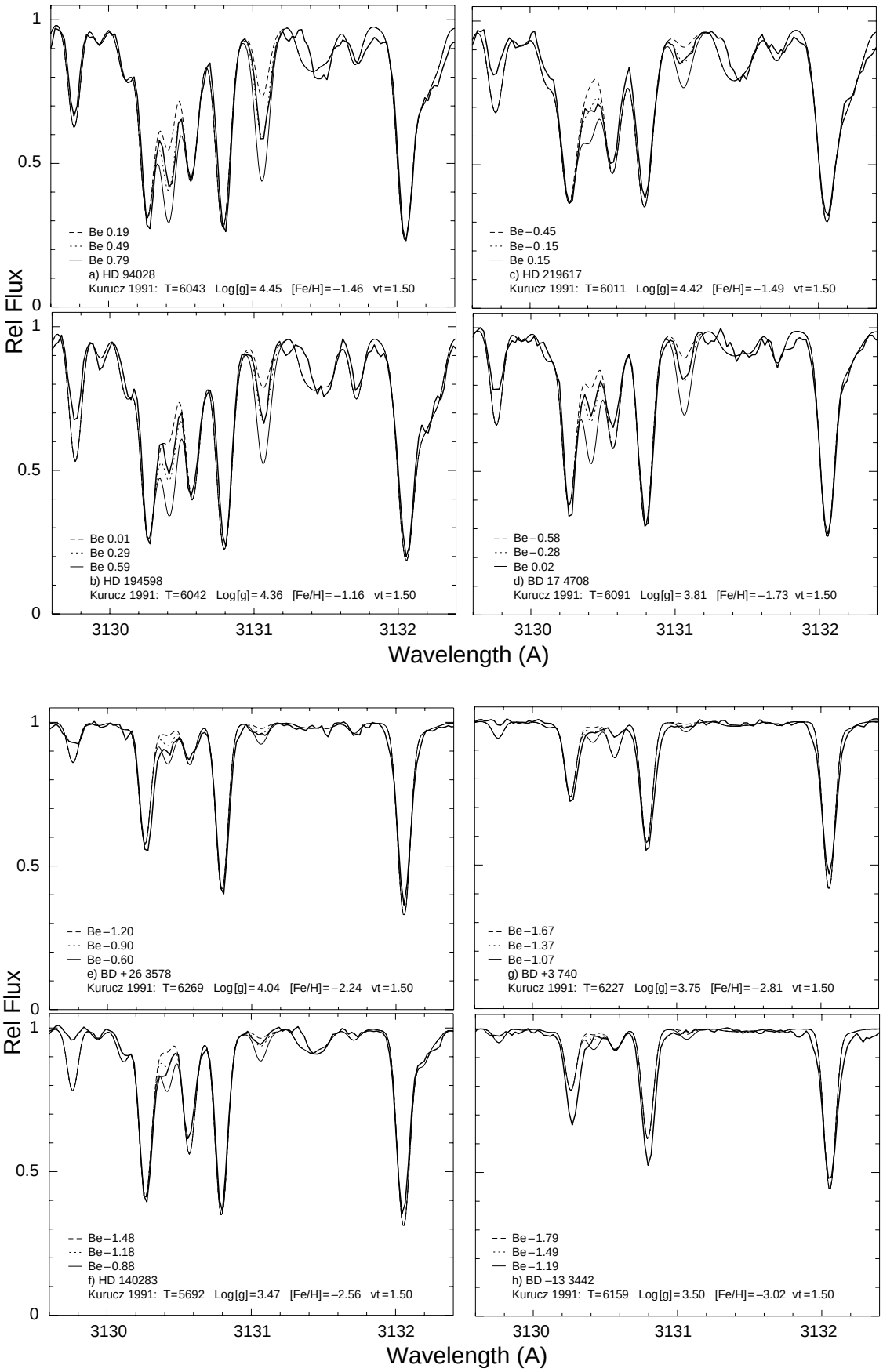

FIG. 3.—Spectrum synthesis fits for eight representative stars. The heavy solid line is the observed spectrum, and the dotted line is the best-fitting synthetic spectrum. The light solid line is the synthetic spectrum with a Be abundance a factor of 2 higher than the best fit, and the dashed line corresponds to a factor of 2 lower than the best fit. The metallicities and the Be abundances are given along with the stellar parameters of the model.

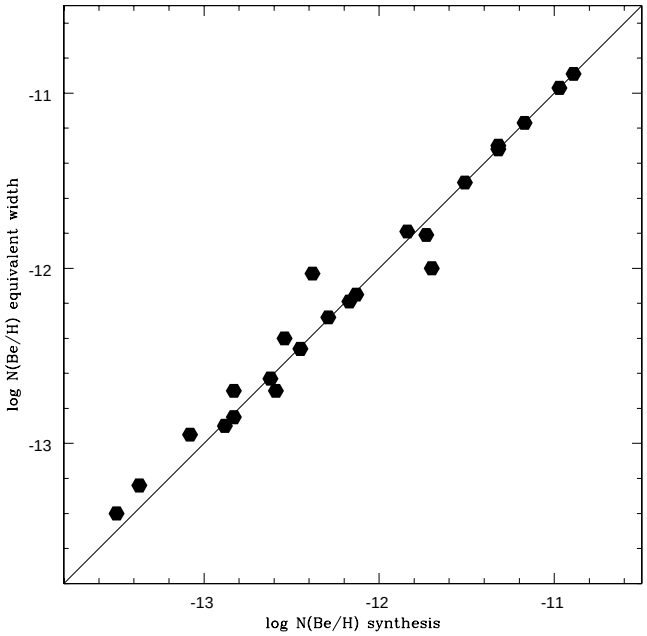

FIG. 4.—Abundance of Be from the equivalent width method compared with that from the synthesis method, for the King scale parameters. The line is the 45° slope. The most discrepant point is our coolest star, HD 103095, which has strong lines, including many molecular lines, and is difficult to fit well.

HD 64090.—The lines in this star are quite strong because of its cool temperature and [Fe/H] $\sim$ 1.7. The shortward Be line is too blended to be used in determining the Be abundance. The fit is good for the longward line, especially for the higher temperature model.

HD 74000.—This star is fairly hot, and the spectrum syntheses match the observed spectrum well. Both Be lines can be used, and the longward line is given twice the weight of the shortward one.

HD 76932.—This spectrum is well synthesized on both temperature scales, and the two Be lines agree quite well.

HD 84937.—The spectrum of this hot, metal-poor star is well matched by the synthetic spectrum on both temperature scales. The two Be lines agree to 0.05 dex. Its spectrum is shown in Figure 1*d*.

HD 94028.—Figure 3*a* shows the spectrum of this star. As can be seen there, its spectrum synthesis is excellent. This is significant because this star lies above the best fit in the Be versus Fe and Be versus O diagrams; it may indicate that there is an intrinsic spread in Be at a given Fe.

HD 103095.—This is the coolest star in our sample, and the synthetic spectra are not good matches to the observed spectrum. There is too much blending to be able to derive a Be abundance with confidence, even though the formal error is small.

HD 134169.—The lines in this star are quite strong ([Fe/H] = −0.9), but the syntheses match the observed spectrum very well. The two Be lines give very similar Be abundances.

HD 140283.—This star is one of the metal-poor standards, and our spectrum has a S/N ratio of 165. Its spectrum is shown in Figures 2*f* and 3*f*. The synthetic fits are good for the parameters on both temperature scales. The 3131 Be line gives a Be abundance that is 0.10 dex lower than the λ3130 line; the weighting is 2:1 for λ3131:λ3130.

HD 184499.—This star has strong lines ([Fe/H] = −0.5) and only the longward Be line could be used in the fit due to heavy blending of the λ3130 line. The λ3131 line is well matched by the synthesis. Its spectrum appears in Figure 2*a*.

HD 194598.—This spectrum can be seen in Figures 2*c* and 3*b*. As Figure 3*b* shows, the synthetic spectrum—on the King scale—is a good match for the observed spectrum, as it is also on the Carney temperature scale.

HD 201889.—The spectrum of this star can be seen in both Figures 1*a* and 2*b*. Both Be lines could be used in the synthesis fits, but, as usual, the abundance from the λ3131 line was given twice the weight as that from the λ3130 line.

HD 219617.—This spectrum and the synthetic fit can be seen in Figure 3*c*. The observed spectrum has a S/N ratio of only 67, but both Be lines were well matched by the synthesis and gave similar results.

BD 37°1458.—The spectrum of this cool, metal-poor star is well matched by the synthetic spectra, and the abundances from the two Be lines agree to 0.04 dex, although the result from the λ3131 line is given a weight of twice that of the λ3130 line.

BD 26°3578.—The spectrum synthesis fit is shown in Figure 3*e*. The spectral features are well represented, and the results from the two Be lines are again weighted 2:1 for λ3131:λ3130.

BD 23°3912.—The region of the Be II lines for this star can be seen in Figure 1*b*. The synthetic spectrum fits yield a well-determined Be abundance. At [Fe/H] = −1.5, this star has distinguished itself by its especially high Li abundance of 2.56 (King, Deliyannis, & Boesgaard 1996). Its Be abundance is normal for its metallicity.

BD 20°3603.—The Be II region of the spectrum of this star is shown in Figure 1*c*. Its metallicity is −2.2, and it is one of the hotter stars in the sample. The synthetic spectrum is an excellent fit, and the Be abundance from the two lines (again, 2:1) is well established.

BD 17°4708.—The spectrum of this star can be seen in Figure 2*d* and its synthesis fit in Figure 3*d*. Both Be lines could be used to evaluate the Be abundance.

BD 3°740.—This star is one of the very lowest metallicity stars in our sample. Its Be spectrum and synthesis fit are presented in Figure 3*g*. Because [Fe/H] = −2.9, the blending lines are weak, and the synthetic spectrum provides a good match. The fits to the two Be lines give the same Be abundance.

BD 2°3375.—The spectrum of this low-metallicity star is well reproduced by our synthetic spectra, and both lines were used to find the Be abundance.

BD −4°3208.—Although the S/N ratio of this spectrum is only 56, because it is a low-metallicity star ([Fe/H] = −2.3), the Be abundance could be found via both Be lines (as weighted 2:1).

BD −13°3442.—This star has the lowest value of [Fe/H]: −3.0. We integrated for a total of 11 hr on this star to achieve a S/N of 129. Its spectrum and the synthesis are shown in Figure 3*h*. It is difficult to make a completely compelling case for Be in this star, and skeptics may consider the abundance we give in Tables 5 and 6 to be an upper limit. There is a strong confirmation of the presence of Be, however; when we fit the strong blending feature at 3130.25 Å with a Gaussian profile and then subtract that Gaussian fit, the remaining line has exactly the correct position for Be II λ3130.42.

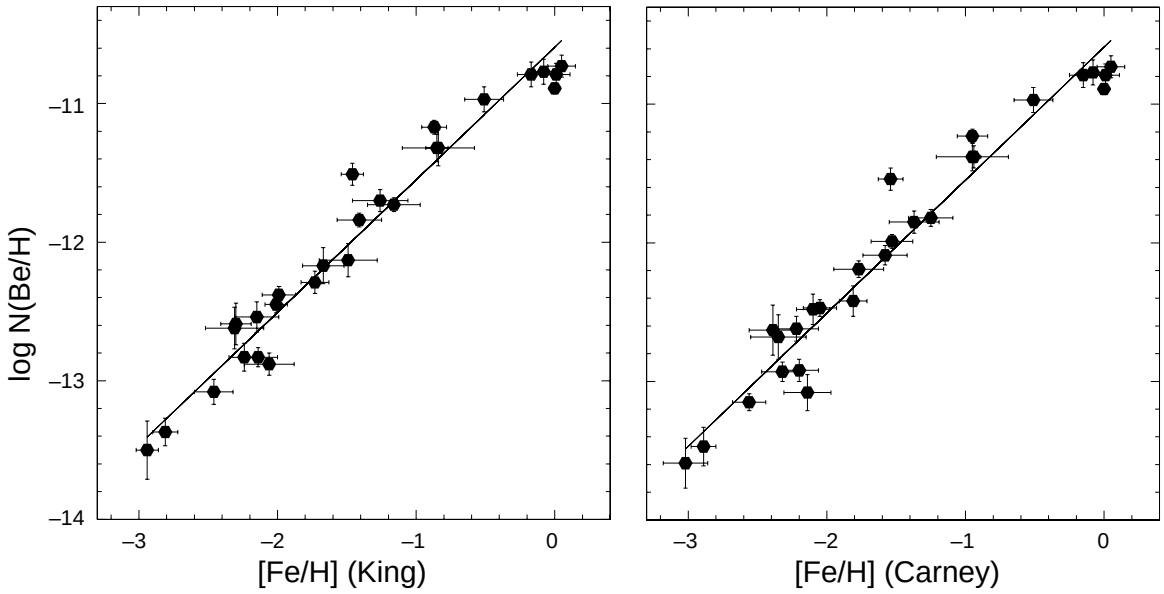

FIG. 5.—Derived Be abundances plotted against [Fe/H] with the derived error bars. The left-hand panel shows the results on the King scale, while the right-hand panel shows the results on the Carney scale. In the solution of the least-squares fit, the error bars in both parameters were taken into account.

HR stars.—The results for these stars have been taken from our prior work (Deliyannis et al. 1998), except for HR 3775, which we have synthesized anew. Its spectrum matches the synthetic spectrum very well, and the two Be II lines give the same Be abundance.

5. DISCUSSION

The key results of this work are the trends of Be with Fe and with O. Figures 5*a* and 5*b* show how Be varies with [Fe/H] on each of the two parameter scales. The line through the points is a least-squares fit that takes the errors in both coordinates into account. The equations for these lines are

$$\log N(\mathrm{Be/H}) = 0.957(\pm 0.038)[\mathrm{Fe/H}] - 10.594(\pm 0.027) \quad \text{(King scale)} ;$$

$$\log N(\mathrm{Be/H}) = 0.960(\pm 0.039)[\mathrm{Fe/H}] - 10.587(\pm 0.027) \quad \text{(Carney scale)} .$$

It appears that Be and Fe increase linearly with a slope near 1.0 for three orders of magnitude in [Fe/H].[2]

We know that there is some intrinsic spread in Be at the metallicities of solar-type stars (Boesgaard & King 1993; Boesgaard et al. 1998), and we may be seeing some evidence of that here at lower metallicities, e.g., at [Fe/H] ~ -1.5 and ~ -2.2. One star stands out above the line at -11.51, -1.46 (King scale) and -11.54, -1.54 (Carney scale); this is HD 94028, and, as mentioned above, the spectrum syntheses are for both sets of stellar parameters are excellent (see Fig. 3*a*). The more straightforward equivalent-width method results in the same Be abundance as the synthesis. When this star is compared to HD 219617, which has the same metallicity, temperature, and log g, the difference in Be is clear: see Figures 3*a* and 3*c*. The derived Be abundances differ by 0.6 dex, or a factor of 4. Thorburn & Hobbs (1996) have also noted the high Be abundance in HD 94028. (They compare this star with HD 194598, which they say is similar in other respects; we find HD 194598 to be a factor of 2 higher in [Fe/H] than HD 94028, and it lies on the "best-fit" line in Figs. 5*a* and 5*b*.) Another pair of stars with similar stellar parameters and different Be abundances is HD 84937 and BD +20°3603; their spectra are shown in Figures 1*c* and 1*d*. Their [Fe/H] values are -2.14 and -2.15 (King scale), and the derived Be abundances differ by 0.3 dex, or a factor of 2. Neither HD 84937 nor HD 94028 stands out from the other stars in terms of its U, V, W velocities or values of apogalacticon distance as given in Carney et al. (1994).

Another interesting star is BD +23°3912 because it has abnormally high Li [A(Li) = 2.56] (King et al. 1996). The Li abundance in this star is a factor of 2–3 above the halo Li plateau. This reflects either (1) an even higher big bang Li abundance, from which all halo stars have depleted to their current level, with this star having suffered less Li depletion than most stars, or (2) Galactic Li production having enriched the material out of which this star formed, from a low ambient (big bang) Li abundance, perhaps near the level of the currently observed plateau. No other elements, including C, O, Al, Na, and several n-capture elements, were found to be abnormal. This seems to rule out a potential Li-producing AGB companion or, for that matter, accretion of material from any source that has undergone either RGB or AGB processing. Unlike Li, Be is not abnormally high in this metal-poor subgiant. The normal Be

[2] A recent paper by Balachandran & Bell (1998) presses the viewpoint that it is necessary to increase the UV opacity in order to make the O abundance in *the Sun* from the UV OH lines match that obtained for the OH IR lines. With the increased UV opacity, the solar Be abundance is then close to the meteoritic value of A(Be) = 1.42. We look forward to a full paper on this subject, which would enable us to evaluate the results better. In the meantime, we suggest that if this effect is real, it might increase the Be abundances of our most metal-rich stars, but have little or no effect on the majority of our abundances which are for stars with [Fe/H] < -1.0. Such an increase for the metal-rich stars would result in a better fit for a single straight line as shown in Figs. 5*a* and 5*b*. However, we also point out that we have derived O abundances for virtually this same set of stars (Boesgaard et al. 1999) and that the O abundance from the IR O I triplet matches those we found from the UV OH lines very well.

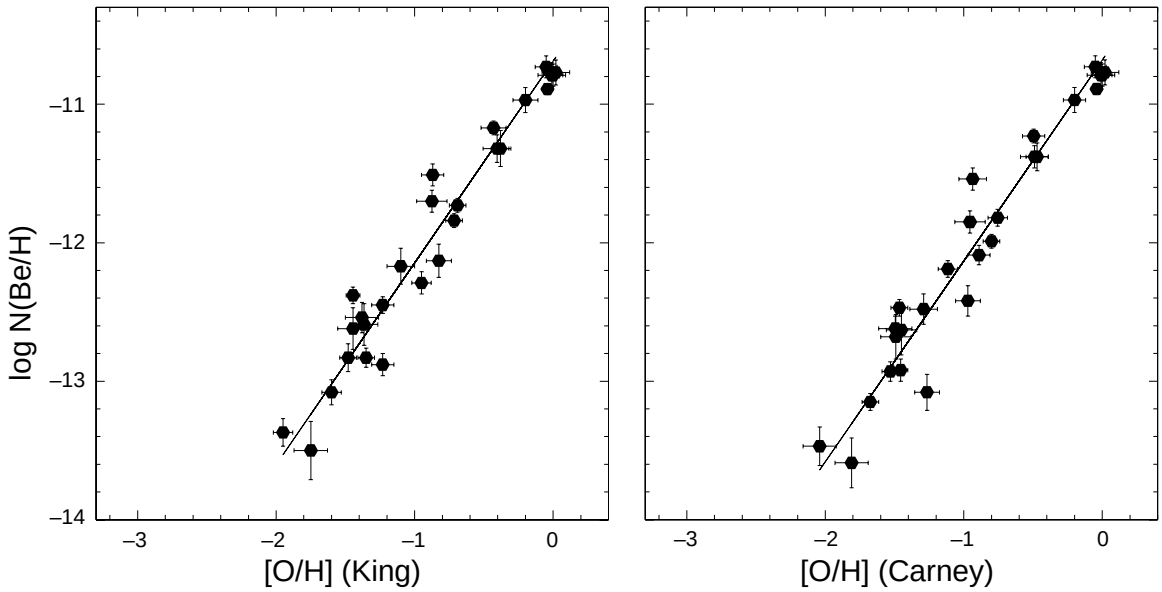

FIG. 6.—Derived Be abundances plotted against [O/H] with the derived error bars. The left-hand panel shows the results on the King scale, while the right-hand panel shows the results on the Carney scale. In the solution of the least-squares fit, the error bars in both parameters were taken into account.

abundance with respect to other little-evolved, near-turnoff stars of similar [Fe/H] suggests that its abnormally high Li abundance is not due to dredge-up of material diffused during the main-sequence lifetime.

Since Be is produced by spallation with CNO nuclei, it is crucial to examine the relationship between Be and O. We have determined O abundances from these same spectra and stellar parameters (Boesgaard et al. 1999). Figures 6*a* and 6*b* show the trend of Be with O; the line through the data points takes into account the errors in both quantities. Again, these are straight-line correlations, represented by

$$\log N(\mathrm{Be/H}) = 1.457(\pm 0.044)[\mathrm{O/H}] - 10.688(\pm 0.044)$$
(King scale) ;

$$\log N(\mathrm{Be/H}) = 1.450(\pm 0.044)[\mathrm{O/H}] - 10.682(\pm 0.043)$$
(Carney scale) .

The relationship between Be and O is well represented by a single straight line. We note that the O abundances are derived in part from our UV spectra where the Be features are; this reduces any systematic trends that might be caused by incorrect UV opacities.

If Be is produced in the ambient interstellar medium by cosmic-ray protons breaking up CNO nuclei, then, in the extreme case, the slope of the relationship between Be and O would be 2. Such a quadratic relationship results from the fact that the number of O atoms is proportional to the cumulative number of SN II's (N), and the number of energetic proton cosmic rays is proportional to the instantanous rate of SN II's (dN). The abundance of the spallation products is therefore the integral of the product $N\,dN = kN^2$. Thus the spallation product (Be) versus O has a slope of 2. Chemical evolution effects, such as an outflow of mass from the halo, indicate that there would be a quadratic relation only at the very lowest metallicities (lower than the present sample) and a progressive shallowing of the slope to disk metallicities. From [Fe/H] between -1 and -2, the slope is close to 1.5. But if Be is produced in the immediate vicinity of the SN II's (the source of both the parent CNO atoms and the cosmic rays), then the slope would be one. The reaction $\mathrm{CNO_{CR}} + \mathrm{H\&He_{ISM}}$ also produces a linear slope, the cosmic-ray CNO being primary (Yoshii et al. 1997). Our Be versus O slope is 1.5. This is consistent with the (traditional) mass outflow model of energetic protons and alpha particles impinging ambient CNO in the ISM but less consistent with either of the linear slope scenarios just described.[3]

In our study of the O abundances we found that there is a strictly linear relationship between Fe and O, over 3 orders of magnitude in Fe, with a slope of 0.66. Now we find a robustly linear relationship between Be and O with a slope of 1.46. These two indicate that the relationship between Be and Fe must also be linear with a slope near 1. This is in fact what we have found in Figures 5*a* and 5*b* where the slope is 0.96.

Nonetheless, we chose to investigate whether there is a change in slope in the Be versus Fe relationship, in part because of the high quality of the data for HD 94028 and in part because the mass outflow models predict a change of slope at disk metallicities. We have tried fitting two lines

[3] The referee raised the issue of what evidence there is of mass outflow in a massive galaxy like ours. In galactic chemical evolution models, physical ejection of gas is not necessary as much as its being lost to the *process* of star formation. Hartwick (1976), for instance, suggested only that it be heated by supernovae so as to prevent further collapse into stars. The apparent need for various amounts of outflow (and inflow) in various galactic chemical evolution models therefore covers a multitude of uncertainties. What is required, of course, is that outflow/inflow invoked in models used to explain halo Fe or O evolution also produces realistic predictions for beryllium evolution.

With halo star formation now having ceased, it is not possible to observe halo mass loss (or heating) directly. However, one might appeal to galactic fountain studies as one source of direct evidence visible today. Moreover, the gravitational potential in the Galactic disk today is probably deeper than that of the fragmentary clouds involved in formation of the halo (Searle & Zinn 1978), and it is not unreasonable to suppose that actual ejection of mass may also have occurred in those halo star-forming regions.

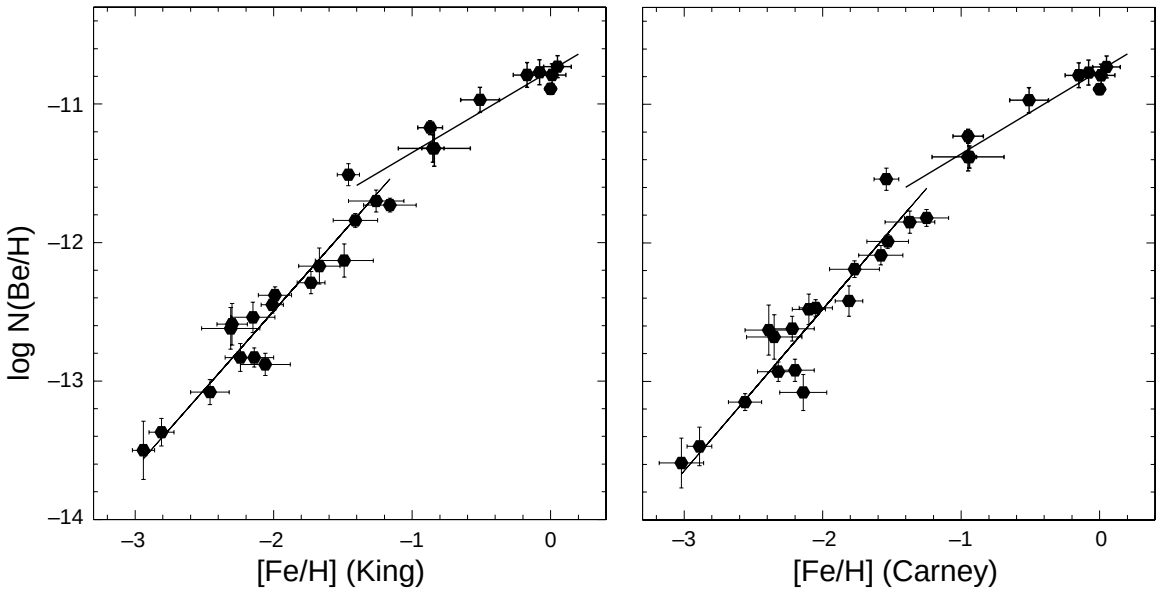

FIG. 7.—Derived Be abundances plotted against [Fe/H] with the derived error bars. The left-hand panel shows the results on the King scale, while the right-hand panel shows the results on the Carney scale. Here two solutions of the least-squares linear fit were made for nine stars with [Fe/H] $\gtrsim -1.0$ and for 18 stars with [Fe/H] $\lesssim -1.1$. The line for the metal-rich solution has been extended artificially to [Fe/H] $= -1.4$.

through the data, one for stars with [Fe/H] $\lesssim -1.1$ and one with [Fe/H] $\gtrsim -1.0$. These fits are shown in Figures 7*a* and 7*b*. (The fit for the metal-rich stars has been extended into the region of lower [Fe/H] stars.) The χ^2 analyses show these to be excellent fits. The two fits for Figure 7*a* are given below.

For the lowest metallicity stars, $-3.0 <$ [Fe/H] < -1.0:

$$\log N(\mathrm{Be/H}) = 1.135(\pm 0.182)[\mathrm{Fe/H}] - 10.225(\pm 0.089) \quad \text{(King scale)} .$$

For the higher metallicity stars, $-1.0 <$ [Fe/H] $< +0.1$:

$$\log N(\mathrm{Be/H}) = 0.592(\pm 0.035)[\mathrm{Fe/H}] - 10.758(\pm 0.079) \quad \text{(King scale)} .$$

The two fits for Figure 7*b* are given below.

For the lowest metallicity stars, $-3.0 <$ [Fe/H] < -1.0:

$$\log N(\mathrm{Be/H}) = 1.167(\pm 0.196)[\mathrm{Fe/H}] - 10.147(\pm 0.094) \quad \text{(Carney scale)} .$$

For the higher metallicity stars, $-1.0 <$ [Fe/H] $< +0.1$:

$$\log N(\mathrm{Be/H}) = 0.602(\pm 0.035)[\mathrm{Fe/H}] - 10.757(\pm 0.070) \quad \text{(Carney scale)} .$$

Our data as seen in Figures 6*a* and 6*b* argue for a single slope to represent the relationships between Be and O (slope 1.45) and perhaps also for Be and Fe (Figs. 5*a* and 5*b*). There seems to be some intrinsic scatter in Be at a given Fe and a given O. Comparably precise data for more stars are needed in order to be more definite about this point.

There is currently no evidence of a Be plateau at abundances down to log N(Be/H) $= -13.5$. Any primordial level predicted by nonstandard BBN must be below that value.

Hoyle, Burbidge, & Narlikar (1993) have proposed a quasi–steady state cosmology with matter creation in ongoing "Planckian fireballs" or "little big bangs." These authors make predictions concerning the light element abundances emerging from these events. The predictions are notable with respect to standard big bang nucleosynthesis in that they predict substantial production of ^{9}Be and ^{11}B. From Table 1 of Hoyle et al., the predicted Be abundance emerging from these creation events is log N(Be/H) ~ -10.5. It can be seen from Figures 5*a*, 5*b*, 6*a*, and 6*b* that our most metal-poor Be abundances are 3 orders of magnitude lower than this value. Given the complete lack of empirical or theoretical evidence suggesting 3 orders of magnitude Be depletion in metal-poor halo stars, our data are difficult to reconcile with the quasi–steady state predictions.

6. CONCLUSIONS

We have obtained high S/N ratio and high-resolution spectra of 27 stars over a range of [Fe/H] of -3.0 to $+0.1$ with the Keck I telescope and HIRES in the blue and ultraviolet spectral region. We have derived Be abundances in these stars from the Be II resonance lines by two methods that are in excellent agreement. One special feature of this work is that our syntheses include the measured enhancement of O found by Boesgaard et al. (1999) for each star. We adopt the results from spectrum synthesis.

In our analysis we have used two different, but plausible, sets of stellar parameters that have been carefully and consistently determined. We have examined the trends of the Be abundance with respect to both the Fe abundance and the O abundance for these stars. The relationships, which take into account the errors in both coordinates, are nearly identical for the two parameter sets.

The linear relation between Be and Fe is

$$\log N(\mathrm{Be/H}) = 0.96(\pm 0.04)[\mathrm{Fe/H}] - 10.59(\pm 0.03) .$$

The linear relation between Be and O is

$$\log N(\mathrm{Be/H}) = 1.45(\pm 0.04)[\mathrm{O/H}] - 10.69(\pm 0.04) .$$

From this we can deduce a general and systematic increase of Be with Fe as the Galaxy evolves. There is a linkage in the formation of Be and O because Be is one of the products from spallation reactions with CNO atoms. However, Be, a trace element, increases much faster than O. As the amount of the abundant element, O, increases by 100 times, Be increases by 800 times.

In traditional models, energetic $\mathrm{H\&He_{CR}}$ interact with ambient CNO in the ISM. When chemical evolution effects such as mass outflow are taken into account, a slope of 1.5 is predicted for halo metallicities. That is, an increase in the number of O nuclei by a factor of 100 implies an increase in the number of Be nuclei by a factor of 1000. By contrast, in the immediate vicinity of a SN II, however, both O atoms (accelerated to high energies) and energetic protons are formed, which in turn form Be. There, the number of Be atoms would be simply proportional to the number of O atoms, and an increase in O by 100 times would be accompanied by an increase in Be by 100 times. Our observed increase in Be of a factor of 800 is therefore consistent with the traditional + mass-outflow models but is less consistent with linear models such as those producing Be in the vicinity of SN II's.

We find some evidence of a spread in the Be abundance at a given O (or Fe) abundance which, if real, indicates that the contributions to Be of an individual star can be somewhat different from star to star. We find no evidence of a plateau in Be at low metallicities, which might be indicative of primordial Be, down to the level of $\log N(\mathrm{Be/H}) = -13.5$.

One of the most important science criteria that determined the optical design of the HIRES spectrograph was that it should have a capability in the deep ultraviolet so we could investigate Be abundances in stars. We started this project during the commissioning run of HIRES in 1993 October. At the time the first author was undergoing chemotherapy for cancer, and she is grateful to Dr. Vogt and Dr. Deliyannis for those observations of five of the halo stars in this paper. Fortunately, she was able to take a major role in the other observations as well as the analyses and interpretation of the Be data. We wish to thank Alex Stephens for his model atmosphere interpolation program and for his help with MOOG. We are grateful to T. Bida at C.A.R.A. for obtaining the spectrum of HD 103095 for us. J. R. K. and C. P. D. acknowledge support from Hubble fellowships, HF-1042.01-93A and HF-1046.01-93A, from the Space Telescope Science Institute, which is operated by the Association of Universities for Research in Astronomy, Inc., under NASA contract NAS 5-26555. The work of A. M. B. has been supported by NSF grants AST 90-16778 and AST-9409793. T. C. B. acknowledges support from NSF grants AST 92-22326 and AST 95-29454.

REFERENCES

Anders, E., & Grevesse, N. 1989, Geochim. Cosmochim. Acta, 53, 197
Balchandran, S., & Bell, R. A. 1998, Nature, 392, 791
Boesgaard, A. M. 1996, in ASP Conf. Ser. 92, Formation of the Galactic Halo...Inside and Out, ed. H. Morrison & A. Sarajedini (San Francisco: ASP), 327
Boesgaard, A. M., Deliyannis, C. P., Stephens, A., & Lambert, D. L. 1998, ApJ, 492, 727
Boesgaard, A. M., & King, J. R. 1993, AJ, 106, 2309
Boesgaard, A. M., King, J. K., Deliyannis, C. P., & Vogt, S. S. 1999, AJ, 117, 492
Boesgaard, A. M., & Steigman, G. 1985, ARA&A, 23, 319
Casuso, E., & Beckman, J. E. 1997, ApJ, 475, 155
Carney, B. W., & Aaronson, M. 1979, AJ, 84, 867
Carney, B. W. 1980, AJ, 85, 38
———. 1983a, AJ, 83, 610
———. 1983b, AJ, 83, 623
Carney, B. W., Latham, D. W., Laird, J. B., & Aquilar, L. A. 1994, AJ, 107, 2241
Chmielewski, Y., Brault, J. W., & Mueller, E. A. 1975, A&A, 42, 37
Copi, C. J., Schramm, D. N., & Turner, M. S. 1995, Science, 267, 192
Deliyannis, C. P., Boesgaard, A. M., King, J. R., & Duncan, D. 1995, in ASP Conf. Ser. 109, New Observations of Beryllium in the Galactic Halo, Ninth Cambridge Workshop on Cool Stars, Stellar Systems, and the Sun, ed. R. Pallavicini & A. Dupree (San Francisco: ASP), 679
———. 1999, in preparation (DBKD)
Deliyannis, C. P., Demarque, P., Kawaler, S. D., Krauss, L. M., & Romanelli, P. 1989, Phys. Rev. Lett., 62, 1583
Deliyannis, C. P., Stephens, A., King, J. R., Boesgaard, A. M., Vogt, S., & Keane, M. 1998, ApJ, 498, L147
Duncan, D. K., Primas, F., Rebull, L. M., Boesgaard, A. M., Deliyannis, C. P., Hobbs, L. M., King, J. R., & Ryan, S. G. 1997, ApJ, 488, 338
Eggen, O. J. 1978, ApJS, 37, 251
Fuhrmann, K., Axer, M., & Gehren, T. 1995, A&A 301, 492
Gilmore, G., Edvardsson, B., & Nissen, P. E. 1991, ApJ, 378, 17
Gilmore, G., Gustafsson, B., Edvardsson, B., & Nissen, P. E. 1992, Nature, 357, 379
Gratton, R. G., Carretta, E., & Castelli, F. 1996, A&A, 314, 191
Gratton, R. G., & Sneden, C. 1988, A&A, 204, 193
Hartwick, F. D. A. 1976, ApJ, 209, 418
Hoyle, F., Burbidge, G., & Narlikar, J. V. 1993, ApJ, 410, 437
Johnson, H. L. 1968, in Stars and Stellar Systems, 7, Nebulae and Interstellar Matter, ed. B. M. Middlehurst & L. M. Aller (Chicago: Univ. Chicago Press), 167
King, J. R. 1993, AJ, 106, 1206
King, J. R., Deliyannis, C. P., & Boesgaard, A. M. 1996, AJ, 112, 2839
———. 1997, ApJ, 478, 778
Kurucz, R. L., Furenlid, I., Brault, J., & Testerman, L. 1984, Solar Flux Atlas from 296 to 1300 nm, NSO Atlas, No. 1 (Sunspot, NM: Natl. Sol. Obs.)
Laird, J. B. 1985, ApJS, 57, 389
Laird, J. B., Carney, B. W., & Latham, D. W. 1988, AJ, 95, 1843
Lemoine, M., Vangioni-Flam, E., & Cassé, M. 1998, ApJ, 499, 735
Magain, P. 1987, A&A, 179, 176
———. 1989, A&A, 209, 211
Malaney, R. A., & Butler, M. N. 1993, ApJ, 407, L73
Malaney, R. A., & Fowler, W. A. 1989, ApJ, 345, L5
Malaney, R. A., & Mathews, G. J. 1992, Phys. Rep., 229, 147
Molaro, P., Bonifacio, P., Castelli, F., & Pasquini, L. 1997, A&A, 319, 593
Orito, M., Kajino, T., Boyd, R. N., & Mathews, G. J. 1997, ApJ 488, 515
Prantzos, N., Cassé, M., & Vangioni-Flam, E. 1993, ApJ, 403, 630
Rebolo, R., Molaro, P., Abia, C., & Beckman, J. E. 1988, A&A, 193, 193
Reeves, H., Fowler, W. A., & Hoyle, F. 1970, Nature, 226, 727
Ryan, S. G. 1989, AJ, 98, 1693
Ryan, S. G., Bessell, M. S., Sutherland, R. S., & Norris, J. E. 1990, ApJ, 348, L57
Ryan, S. G., Norris, J. E., Bessell, M. S., & Deliyannis, C. P. 1992, ApJ, 388, 184
Schuster, W. J., & Nissen, P. E. 1988, A&AS, 73, 275
Searle, L., & Zinn, R. 1978, ApJ, 225, 357
Sneden, C. 1973, ApJ, 184, 839
Steffen, M. 1985, A&AS, 59, 403
Thomas, D., Schramm, D., Olive, K., Mathews, G. J., Meyer, B. S., & Fields, B. D. 1994, ApJ, 430, 291
Thorburn, J. A., & Hobbs, L. M. 1996, AJ, 111, 2106
Tomkin, J., & Lambert, D. L. 1978, ApJ, 223, 937
Tomkin, J., Lemke, M., Lambert, D. L., & Sneden, C. 1992, AJ, 104, 1568
Vangioni-Flam, E., Audouze, J., Oberto, Y., & Cassé, M. 1990, ApJ, 364, 568
Vangioni-Flam, E., Ramaty, R., Olive, K., & Cassé, M. 1998, A&A, 337, 714
Vogt, S. S., et al. 1994, Proc. SPIE, 2198, 362
Walker, T. P., Steigman, G., Schramm, D. N., Olive, K. A., & Kang, H.-S. 1991, ApJ, 376, 51.
Witten, E. 1984, Phys. Rev. D, 30, 272
Yoshii, Y., Kajino, T., & Ryan, S. G. 1997, ApJ, 485, 605